Biomacromolecules

Article

Cite This: Biomacromolecules 2020, 21, 240−249

pubs.acs.org/Biomac

Light-Activated, Bioadhesive, Poly(2-hydroxyethyl methacrylate) Brush Coatings

Jian Wang,[†] Peyman Karami,[‡] Nariye Cavusoglu Ataman,[†] Dominique P. Pioletti,[‡] Terry W. J. Steele,[§] and Harm-Anton Klok*[,†,§]

[†]Institut des Matériaux and Institut des Sciences et Ingénierie Chimiques, Laboratoire des Polymères, École Polytechnique Fédérale de Lausanne (EPFL), Bâtiment MXD, Station 12, CH-1015 Lausanne, Switzerland

[‡]Laboratory of Biomechanical Orthopedics, Institute of Bioengineering, École Polytechnique Fédérale de Lausanne (EPFL), CH-1015 Lausanne, Switzerland

[§]School of Materials Science and Engineering, Nanyang Technological University, 50 Nanyang Avenue, Singapore 639798, Singapore

Supporting Information

ABSTRACT: Rapid adhesion between tissue and synthetic materials is relevant to accelerate wound healing and to facilitate the integration of implantable medical devices. Most frequently, tissue adhesives are applied as a gel or a liquid formulation. This manuscript presents an alternative approach to mediate adhesion between synthetic surfaces and tissue. The strategy presented here is based on the modification of the surface of interest with a thin polymer film that can be transformed on-demand, using UV-light as a trigger, from a nonadhesive into a reactive and tissue adhesive state. As a first proof-of-concept, the feasibility of two photoreactive, thin polymer film platforms has been explored. Both of these films, colloquially referred to as polymer brushes, have been prepared using surface-initiated atom transfer radical polymerization (SI-ATRP) of 2-hydroxyethyl methacrylate (HEMA). In the first part of this study, it is shown that direct UV-light irradiation of PHEMA brushes generates tissue-reactive aldehyde groups and facilitates adhesion to meniscus tissue. While this strategy is very straightforward from an experimental point of view, a main drawback is that the generation of the tissue reactive aldehyde groups uses the 250 nm wavelength region of the UV spectrum, which simultaneously leads to extensive photodegradation of the polymer brush. The second part of this report outlines the synthesis of PHEMA brushes that are modified with 4-[3-(trifluoromethyl)-3*H*-diazirin-3-yl]benzoic acid (TFMDA) moieties. UV-irradiation of the TFMDA containing brushes transforms the diazirine moieties into reactive carbenes that can insert into C−H, N−H, and O−H bonds and mediate the formation of covalent bonds between the brush surface and meniscus tissue. The advantage of the TFMDA-modified polymer brushes is that these can be activated with 365 nm wavelength UV light, which does not cause photodegradation of the polymer films. While the work presented in this manuscript has used silicon wafers and fused silica substrates as a first proof-of-concept, the versatility of SI-ATRP should enable the application of this strategy to a broad range of biomedically relevant surfaces.

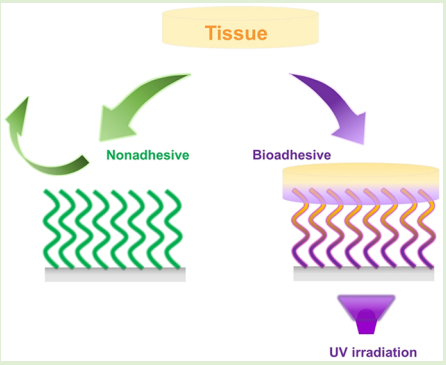

INTRODUCTION

Rapid adhesion between tissue interfaces or between tissue and synthetic materials is sought after clinically to accelerate wound healing and facilitate the integration of implantable medical devices and biosensors. Sutures and staples are widely used to mediate tissue fixation. The use of these mechanical techniques, however, can damage surrounding tissue and lead to scar formation. One way to overcome these drawbacks is the use of bioadhesive materials that can form (covalent) chemical bonds with the tissue.[1−3]

A number of bioadhesive material platforms, which can chemically mediate tissue adhesion, have been developed.[4−11] These include both synthetic polymeric materials, most notably cyanoacrylates, but also PEG-based systems, as well as biological polymers such as fibrin. Each of these systems has distinguished advantages, but also specific limitations. Cyanoacrylate-based adhesives, for example, provide relatively high adhesion strengths, but are brittle and relatively inflexible. Fibrin and PEG-based adhesives, in contrast, provide a soft interface, but generally only provide limited adhesive strength.

Most of the adhesive materials discussed above are applied as one or two component formulations in the form of a viscous liquid. This only provides limited control over the amount of material that is applied and, thus, over the thickness of the

Special Issue: Future of Biomacromolecules at a Crossroads of Polymer Science and Biology

Received: August 29, 2019
Revised: October 7, 2019
Published: October 9, 2019

adhesive layer. In the case of two-component formulations, specialized delivery syringes are required that allow the mixing of the two components immediately before application. Another challenge with many bioadhesives is that network formation and interfacial bonding set in as soon as the two components of the adhesive are mixed and brought into contact with the tissue. As a consequence, precise control of the activation of the adhesive is limited, which makes it difficult to reposition or readjust the tissue−tissue or tissue−device interface after application of the adhesive. One way to overcome this limitation is to use external stimuli to trigger interfacial bonding. Light is an attractive and powerful stimulus, as it potentially allows to control adhesion in time and space. A number of reports have been published that describe light-activated tissue adhesives.[12−21] Often, UV light is used to initiate network formation and interfacial bonding.[13−17,21] In other cases, UV-irradiation has been used to convert nonreactive, nonadhesive functional groups, such as diazirines, into carbene moieties that can react to form covalent bonds with the tissue.[12,18−20]

Most of the light-activated adhesives that have been reported so far are applied as a gel or as a liquid formulation. One interesting exception is a study in which photoreactive diazirine moieties were attached to amine-functionalized PLGA substrates.[12] Upon photoirradiation, diazirines generate carbenes that can insert in C−H, N−H, and O−H bonds present in tissue. While this work demonstrated the feasibility of the diazirine motif to photochemically mediate the formation of robust, covalent bonds with tissue, the specific system also suffers from a number of limitations. One drawback is the relatively hydrophobic nature of the PLGA film, which impedes effective wetting of the tissue. Another limitation is the rigid nature of the PLGA substrate, which hampers the establishment of close, interfacial contact between the tissue and the synthetic material. One possible, general strategy to alleviate these challenges is to modify the substrate of interest with a thin, water-swellable, and soft polymer thin film, which provides conformal contact with the tissue surface and is modified with functional groups that can be transformed on-demand using, for example, light from nonadhesive to tissue reactive and, thus, adhesive. This article explores the feasibility of this strategy, using thin, chain-end tethered polymer coatings, polymer brushes, prepared via surface-initiated atom transfer radical polymerization (SI-ATRP) as a model system. SI-ATRP is an attractive method to prepare these systems, as it provides relatively good control over the molecular weight of the surface-grafted polymer (and, thus, film thickness), as well as the chemical composition and functionality of the resulting polymer films.[22,23] The polymer brushes investigated in this study were obtained by SI-ATRP of 2-hydroxyethyl methacrylate (HEMA). This monomer was selected since polymer brushes containing side chain ethylene glycol functional groups such as PHEMA and poly(poly(ethylene glycol methacrylate)) (PPEGMA) are well-known for their ability to prevent nonspecific adsorption of proteins, cells, and bacteria, as well as fungi.[24−28] PHEMA brushes as a consequence, thus, represent an attractive, nonbioadhesive model polymer coating. To convert these nonbioadhesive PHEMA brushes into tissue-binding coatings, two light-mediated strategies have been explored. A first strategy involves direct irradiation of a PHEMA brush film with UV-light. The second strategy uses PHEMA brushes that have been postmodified to introduce photoreactive diazirine moieties. For each of these two classes of photoactive brush coatings, this manuscript presents the synthesis and characterization of the brush films as well as their evaluation as bioadhesive coatings in experiments that use bovine meniscus tissue.

EXPERIMENTAL SECTION

Materials. All chemicals were used as received unless described otherwise. Copper(I) chloride (99.999%), copper(II) bromide (99.999%), copper(I) bromide (99.995+%), 2,2′-bipyridyl (bpy) (99%), 2-bromo-2-methylpropionyl bromide, chlorodimethylsilane (98%), dimethyl sulfoxide (DMSO, 99.5%), aniline (99.5%), *N*,*N*′-dicyclohexylcarbodiimide (DCC, 99%), 4-(dimethylamino)pyridine (DMAP, 99%), 2-hydroxyethyl methacrylate (HEMA, 97%), and 2-methacryloyloxyethyl phosphorylcholine (MPC, 97%) were purchased from Sigma-Aldrich. Before use, MPC was washed with cold acetonitrile to remove the inhibitor, filtered, and dried under vacuum. HEMA was freed from the inhibitor by passing through a column of activated, basic aluminum oxide and distilled prior to use. Aniline was distilled before use. 4-[3-(Trifluoromethyl)-3*H*-diazirin-3-yl]benzoic acid (TFMDA, 98%) was purchased from TCI. Acetic anhydride was purchased from Fluka. The ATRP initiator (6-(2-bromo-2-methyl)-propionyloxy)hexyldimethylchlorosilane was synthesized as previously reported.[29] Methanol (MeOH) was purchased from Alfa Aesar. Triethylamine was purchased from Aldrich and distilled over KOH before use. Dichloromethane (DCM) and toluene were purified and dried using a solvent-purification system (PureSolv). Deionized water was obtained from a Millipore Direct-Q 5 water purification system. For adhesion studies, polymer brushes were grown from fused silica wafers, which had been cut into rectangular slides of ∼1.5 cm × 1.5 cm. Ellipsometry and X-ray photoelectron spectroscopy (XPS) analyses were performed on polymer brushes, which were prepared using 0.8 cm × 1 cm rectangular silicon substrates. Samples for UV−vis analysis were grafted from 0.8 cm × 1 cm rectangular fused silica substrates. Tissue specimens were harvested from mature bovine knee joints procured from the local abattoir shortly after slaughter of the animals (12−18 months of age). Before sample preparation, the isolated tissue was washed in PBS, which was obtained from Thermo Fisher Scientific.

Analytical Methods. XPS was carried out using an Axis Ultra instrument from Kratos Analytical equipped with a conventional hemispheric analyzer. The X-ray source employed was a monochromatic Al Kα (1486.6 eV) source operated at 100 W and 10^{-9} mbar. Surfaces were cleaned with a Femto O_2 Plasma system (200 W, Diener Electronic). Dry film thicknesses were determined using a SemiLAB (SE2000) ellipsometer and calculated based on a four-layer silicon/silicon oxide/polymer brush/air model, assuming the polymer brush to be isotropic and homogeneous. A Hamamatsu Lightningcure L8858−02, 200 W UV lamp was used as the light source. The spectral characteristics of this UV lamp, which has a center wavelength of 365 nm, are included in Supporting Information, Figure S1. For some experiments, a Mercury Line Bandpass Filter with a center wavelength of 365 ± 2 nm was used to block lower wavelength UV light (in particular, the ∼250 nm wavelength band). UV−visible absorbance spectra were recorded using a Varian Cary 100 Bio UV−visible spectrophotometer at room temperature. Attenuated total reflectance Fourier transform infrared (ATR-FTIR) spectroscopy was carried out on a Nicolet 6700 FT-IR spectrometer from Thermo Scientific.

PROCEDURES

Preparation of ATRP Initiator-Modified Silica and Fused Silica Surfaces. Silica and fused silica surfaces were first sonicated in ethanol, water, and acetone (5 min each). The substrates were dried under a flow of nitrogen and exposed to oxygen plasma for 20 min. After that, the substrates were transferred immediately to a reactor containing a 10 mM solution of (6-(2-bromo-2-methyl)propionyloxy)-hexyldimethylchlorosilane in dry toluene under nitrogen

DOI: 10.1021/acs.biomac.9b01196
Biomacromolecules 2020, 21, 240−249

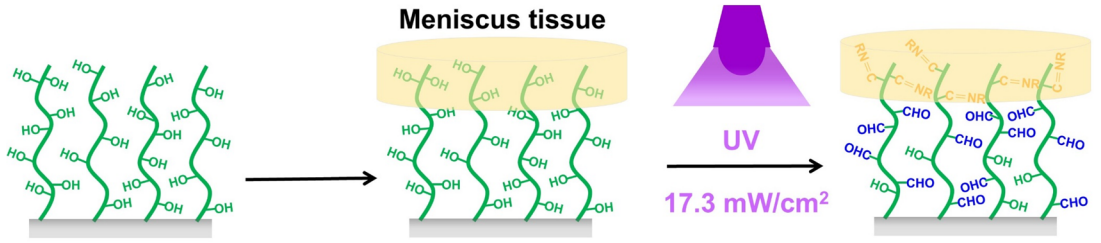

Figure 1. Schematic illustration of the UV-activation of PHEMA brushes and subsequent adhesion to meniscus tissue.

atmosphere. The reaction was allowed to proceed for 16 h at room temperature after which the modified surfaces were removed and washed extensively with toluene, ethanol and DCM. All substrates were dried under a flow of nitrogen and subsequently transferred to a reactor for SI-ATRP.

Surface-Initiated Atom Transfer Radical Polymerization of 2-Hydroxyethyl Methacrylate (HEMA). Surface-initiated atom transfer radical polymerization of HEMA was carried out following an established protocol.[30]

Surface-Initiated Atom Transfer Radical Polymerization of 2-Methacryloyloxyethyl Phosphorylcholine (MPC). MPC (6.65 g, 22.5 mmol) was placed in a Schlenk tube under nitrogen atmosphere. The Schlenk tube was subsequently evacuated and filled with nitrogen three times. Then, 2,2′-bipyridyl (bpy) (140.5 mg, 0.9 mmol), $CuBr_2$ (10.05 mg, 0.045 mmol) and a methanol/water solution (4:1, v:v, 15 mL) were added into another Schlenk tube. After three freeze/pump/thaw cycles, the solution was frozen. Then, CuBr (64.5 mg, 0.45 mmol) was added under a nitrogen flow, and the frozen solution was thawed. The molar ratio of MPC/CuBr/$CuBr_2$/bpy in the reaction mixture was 50:1:0.1:2. The mixture was stirred under nitrogen and briefly sonicated to completely dissolve the CuBr. After an additional freeze/pump/thaw cycle, the resulting ATRP solution was cannula transferred to a Schlenk tube containing the MPC powder. After complete dissolution of MPC, the reaction mixture was cannula transferred to nitrogen-purged glass vials containing an initiator-functionalized substrate. After 15 h, the substrate was removed from the ATRP solution, extensively rinsed with methanol, water, and ethanol and finally dried under a flow of N_2.

Albright-Goldman Oxidation of PHEMA Brushes. The postpolymerization oxidation of PHEMA brushes was performed following a previously published protocol.[31]

Aniline Labeling of the Aldehyde-Functionalized PHEMA Brushes. Aniline labeling of aldehyde-functionalized PHEMA brushes was performed following a previously published protocol with slight modifications.[32] Instead of poly(poly(ethylene glycol) methacrylate) (PPEGMA) brush-coated substrates and a reaction time of 24 h, aldehyde-functionalized PHEMA brushes were used, which were incubated in 10 mL of an ethanol solution containing 1 mL of aniline for 5 h.

Postpolymerization Modification of PHEMA Brushes with TFMDA. Postpolymerization modification of PHEMA brushes with TFMDA was performed by using a previously published protocol with slight modifications.[33] In a typical experiment, 92 mg (0.08 mmol) TFMDA and 107.2 mg (0.88 mmol) DMAP were dissolved in 24 mL dry DCM. The resulting solution was transferred to a nitrogen purged reaction vessel containing the PHEMA modified surfaces in 16 mL of a DCM solution containing 91.2 mg (0.44 mmol) DCC. After stirring the reaction solution at 0 °C for 5 min and subsequently 1 or 16 h at room temperature, substrates were washed extensively with DCM and ethanol and dried under a flow of nitrogen. TFMDA concentrations ($[c]$) were calculated according to the Beer–Lambert law, $A = \varepsilon \cdot l \cdot [c]$, where "$A$" is the measured absorbance, "ε" is the calculated molar extinction coefficient, and "l" is the polymer brush thickness.

Adhesion Testing. The adhesive performance of the brush-coated substrates was evaluated in the tensile mode, as schematically illustrated in Figure S2, against fresh bovine meniscus tissue. Cylindrical discs with a diameter of 6.8 mm were cut in the circumferential direction from the central region of the bovine lateral meniscus and then glued onto a metal support using cyanoacrylate glue (LOCTITE 401). The brush-coated fused silica samples were placed on top of the tissue surface and then exposed to UV illumination with an intensity of 17.3 mW/cm^2 at 365 nm for a defined period. Directly after illumination, the samples were mounted into an Instron E3000 linear mechanical testing machine (Norwood, MA, U.S.A.) equipped with a 50 N load cell. Tests were performed with a constant speed of 0.5 mm·s^{-1} at room temperature and the applied force was recorded. The adhesion strength was determined by dividing the maximum detected force by the surface area of the meniscus. As an example, Figure S3 illustrates this experiment using a PHEMA brush with a dry thickness of 145 nm that was exposed to UV light for 3 min. Tests were performed until failure at the polymer brush–tissue interface. Each test was performed with at least five replicates. For adhesion tests on PHEMA-coated substrates, which were activated by Albright-Goldman oxidation, the brush-modified substrates were placed on top of and in contact with the tissue for 3 min without UV irradiation.

Statistical Analysis. Tensile adhesion data are presented as the mean ± standard deviation across samples. Statistical analysis was performed using one-way ANOVA. A p-value < 0.05 was considered statistically significant.

RESULTS AND DISCUSSION

The manuscript investigates the feasibility of two light-activated polymer brush-based bioadhesive coatings. First, the preparation, characterization, and bioadhesive properties of coatings obtained by direct UV-irradiation of PHEMA brushes will be presented. After that, a second approach toward light-activated polymer brushes, which are obtained by postpolymerization modification of PHEMA films with photoreactive diazirine moieties will be discussed.

Direct UV-Activation of PHEMA Brushes. The first strategy toward light-activated polymer-based bioadhesive surfaces is based on the direct UV-irradiation of PHEMA brushes (Figure 1). PHEMA and other side chain ethylene glycol substituted polymethacrylate brushes are well-known for

DOI: 10.1021/acs.biomac.9b01196
Biomacromolecules 2020, 21, 240–249

Scheme 1. Synthesis of PHEMA Brushes via SI-ATRP

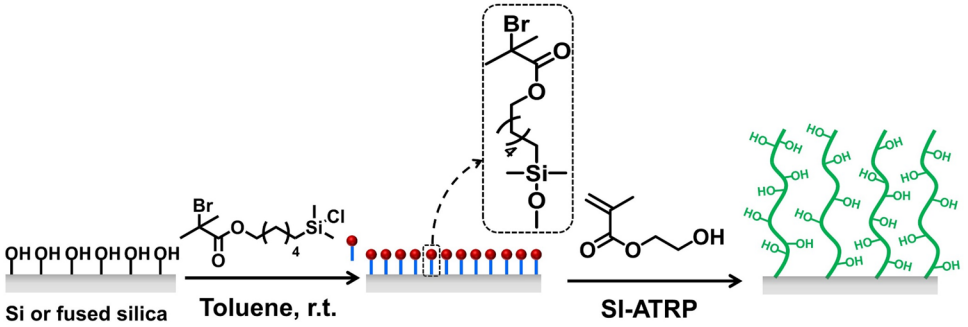

their ability to prevent the nonspecific adsorption of proteins, cells, bacteria, and fungi.[24−28] It has also been shown that irradiation of PPEGMA brushes, as well as oligo(ethylene glycol) terminated self-assembled monolayers with ∼250 nm UV light generates functional groups, presumably aldehydes, which have been used to covalently bind proteins.[34−39] Covalent immobilization of proteins on aldehyde surfaces involves the formation of imine bonds that are generated by reaction between aldehyde groups and amine groups in proteins. As the tissue extracellular matrix is rich in amine groups, this suggests that the photochemical reactivity of PHEMA or PPEGMA brushes may not only be explored to allow light-controlled protein immobilization, but may possibly also be harnessed to create on-demand, light-activated tissue-adhesive thin polymer interfaces. To explore the feasibility of this concept, PHEMA brushes with a dry film thickness of 145 nm were grown from silicon wafers or fused silica substrates via SI-ATRP, as outlined in Scheme 1. As a control, putatively nonphotoreactive control coating, poly(2-methacryloyloxyethyl phosphorylcholine) (PMPC) brushes with a dry film thickness of 154 nm were used, which were also produced via SI-ATRP. PMPC brushes are also very effective non-biofouling surface coatings,[40−42] but in contrast to PHEMA brushes, do not produce tissue reactive groups upon UV-irradiation (vide infra).

The ability of the PHEMA brushes to act as on-demand, light-activated adhesive coatings was investigated using meniscus tissue. Details of the experimental setup are provided in Figure S2. PHEMA brushes with a dry film thickness of 145 nm grown from fused silica substrates were placed in contact with the meniscus tissue and subsequently irradiated with UV light for a defined period of time. After that, adhesion strengths were determined at room temperature using a 50 N load at a constant speed of 0.5 mm·sec^{-1}. The adhesive properties of the UV-activated PHEMA brushes were compared with those of 154 nm thick PMPC brushes that were subjected to UV-irradiation under the same conditions. As a second control, PHEMA brushes with a dry film thickness of 191 nm were used, which were not activated by UV-irradiation, but instead were treated with DMSO/acetic anhydride before being put in contact with the meniscus tissue. The use of DMSO/acetic anhydride ("Albright−Goldman oxidation") represents a wet-chemical strategy that has been used previously to convert hydroxyl side chain functional groups of PHEMA brushes into aldehyde moieties.[31]

Figure 2 compares the adhesion strengths that were measured on untreated PHEMA brushes with those exposed to UV-irradiation for 1 or 3 min, as well as on the PMPC and wet-chemically oxidized PHEMA brush control samples. The

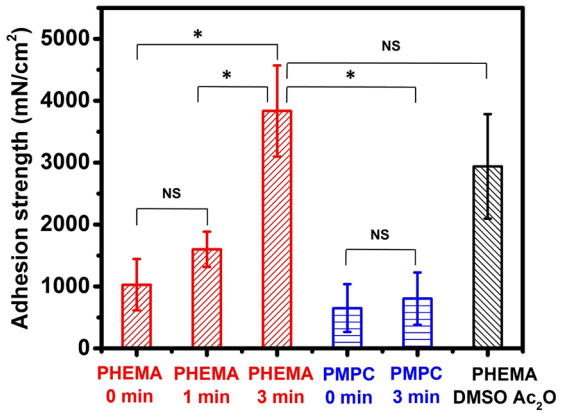

Figure 2. Adhesion strengths of PHEMA brush coated substrates (d = 145 nm) treated with UV light for 0, 1, and 3 min (red), PMPC brush-coated substrates treated with UV light for 0 and 3 min (blue) and DMSO Ac_2O-activated PHEMA brush-coated substrates (black). Asterisks indicate statistically significant differences whereas NS represent not significant difference between two conditions. Significant at *$p < 0.05$.

results summarized in Figure 2 show that the adhesion strengths of the PHEMA brushes increase upon UV-light irradiation and that increasing the duration of the UV treatment leads to a further, significant increase of the adhesion strength. The adhesion strengths that were measured on the UV-activated PHEMA brush films compare well with those that have been reported for fibrin glue and synthetic polymer adhesives, which were applied in a conventional way as a liquid/gel formulation on meniscus tissue.[43−45] The adhesion strengths recorded on the nonirradiated, control PHEMA brushes were comparable to those measured on the PMPC brushes. UV-irradiation of the PMPC brushes did not result in a change in the adhesion strength. Finally, the adhesion strengths measured on PHEMA brushes, which were subjected to UV-irradiation for 3 min, were comparable to those determined on PHEMA brush films that were activated via Albright-Goldman oxidation. This last observation is consistent with the formation of aldehyde groups upon UV-irradiation of the PHEMA brushes.

Next, a number of experiments were carried out to elucidate the effect of UV-irradiation on the chemical composition and structure of the PHEMA brushes. First, a 145 nm thick PHEMA brush grafted from a silicon substrate was subjected to UV-irradiation for 3 min and subsequently analyzed by XPS and ellipsometry. Figure 3A compares the XPS C_{1s} high resolution scans that were recorded on the brush prior to and after the 3 min irradiation time. Most prominent is the

DOI: 10.1021/acs.biomac.9b01196
Biomacromolecules 2020, 21, 240−249

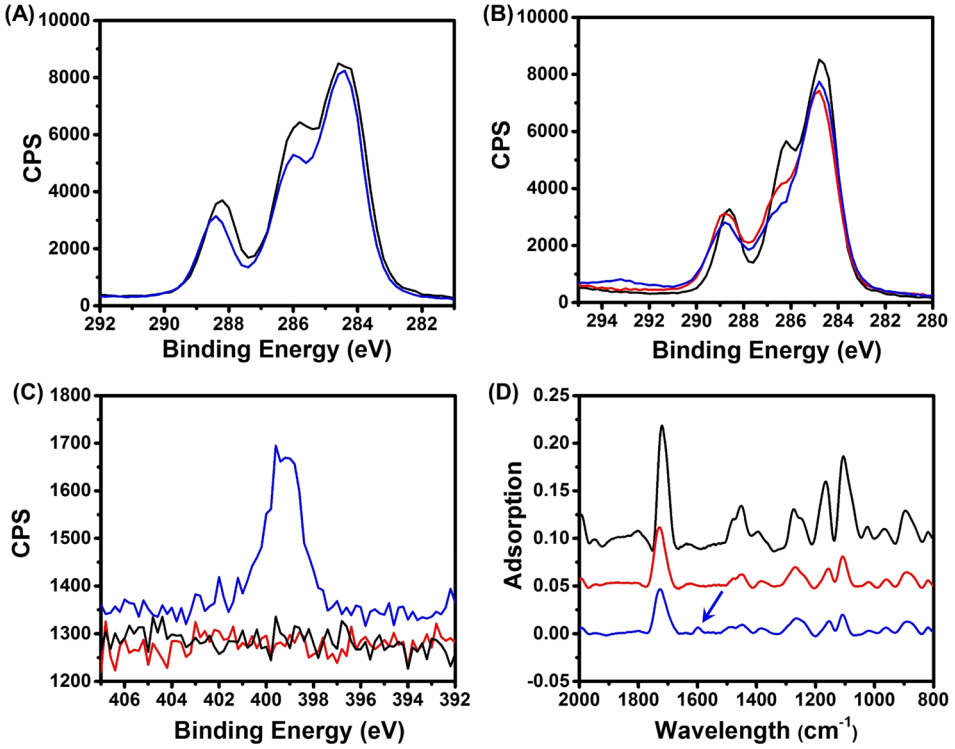

Figure 3. (A) C_{1s} high resolution XPS spectra of a PHEMA brush coated substrate before (black) and after treated with UV irradiation for 3 min (blue), (B) C_{1s} and (C) N_{1s} high resolution XPS scans of a PHEMA brush coated substrate (black), a DMSO/Ac_2O-activated PHEMA brush-coated substrate (red) and an aniline-labeled aldehyde-functionalized PHEMA brush-coated substrate (blue). (D) FTIR spectra of a PHEMA brush-coated substrate (black), a DMSO/Ac_2O-activated PHEMA brush-coated substrate (red) and an aniline-labeled aldehyde-functionalized PHEMA brush-coated substrate (blue).

decrease in the intensity of the shoulder at 285.9 eV, which is indicative of changes in the chemical composition of the brush upon UV-irradiation. Ellipsometric analysis of the PHEMA brush revealed a decrease in film thickness from 145 to 75 nm indicating that these changes in chemical structure are accompanied by partial photodegradation of the brush film. The observed changes in chemical composition as well as the partial photodegradation are in agreement with the results of previous work in which 250 nm wavelength UV-laser light was used to generate protein-patterned PPEGMA brushes.[34−39] In contrast, when the PHEMA brush was subjected to UV light using a bandpass filter that removes the lower wavelength band around 250 nm, no changes in the C_{1s} high resolution XPS scans were observed (Figure S4) and the film thickness remained constant. This indicates that it is the lower wavelength, UV−C part of the light spectrum of the light source that is responsible for the photoactivation and−degradation of the PHEMA brushes.

Figure 3B−D shows XPS high-resolution scans and FTIR spectra recorded on PHEMA brush samples that were activated by Albright-Goldman oxidation. To illustrate the reactivity of the activated brushes toward amines, these films were also treated with aniline, which served as a model amine. Comparison of the C_{1s} high resolution scans taken from PHEMA brushes before and after Albright-Goldman oxidation (Figure 3B) reveals changes that are similar to those in Figure 3A, which is a further indication that UV-irradiation of PHEMA brushes results in the formation of tissue-reactive aldehyde groups. Figure 3C,D shows N_{1s} high-resolution XPS scans and FTIR spectra of aldehyde-functionalized PHEMA brushes generated via Albright-Goldman oxidation before and after reaction with aniline. The N_{1s} high-resolution XPS scan recorded after the reaction reveals a signal at 398.9 eV, which is consistent with the formation of an imine bond upon reaction of aniline with the side chain aldehyde groups in the brush (Figure 3C).[46,47] Furthermore, the FTIR spectra in Figure 3D indicate the appearance of a small, new peak at 1600 cm^{-1} after aniline labeling, which can be assigned to the C−C stretching vibrations of the aromatic aniline ring. In addition to the PHEMA brushes, also the influence of UV-irradiation on the PMPC control samples was studied. As for the PHEMA brushes, UV-irradiation was found to result in partial photodegradation. For the PMPC brushes, 3 min of UV-irradiation resulted in a decrease in film thickness from 154 to 32 nm. Figure S5, finally, compares XPS spectra of the PMPC brushes before and after UV-irradiation. In contrast to the PHEMA brushes, these spectra do not indicate any changes in the chemical composition of the PMPC brushes.

Taken together, the results presented above indicate that direct UV-irradiation of PHEMA brushes provides a way to convert these polymer films, which are generally considered nonbiofouling, into tissue-reactive adhesives. The model studies discussed in the previous paragraph indicate that the UV-irradiation generates aldehyde groups and that it is the lower wavelength part of the UV-spectrum that is responsible for these photochemical changes.

UV-Activation of Diazirine Functionalized Brushes. The work described above demonstrates that direct UV-irradiation of PHEMA brushes allows to introduce amine-reactive groups into these polymer thin films and transforms these otherwise nonfouling coatings into bioadhesive surfaces. While the data presented in Figure 2 show that this approach

DOI: 10.1021/acs.biomac.9b01196
Biomacromolecules 2020, 21, 240−249

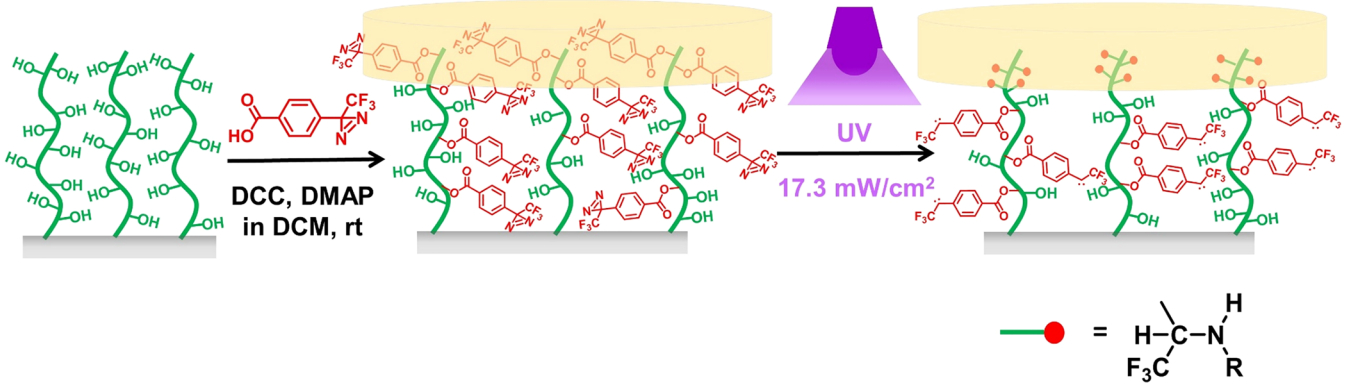

Figure 4. Postpolymerization modification of a PHEMA brush-coated substrate with TFMDA and subsequent photoactivation and adhesion to meniscus tissue.

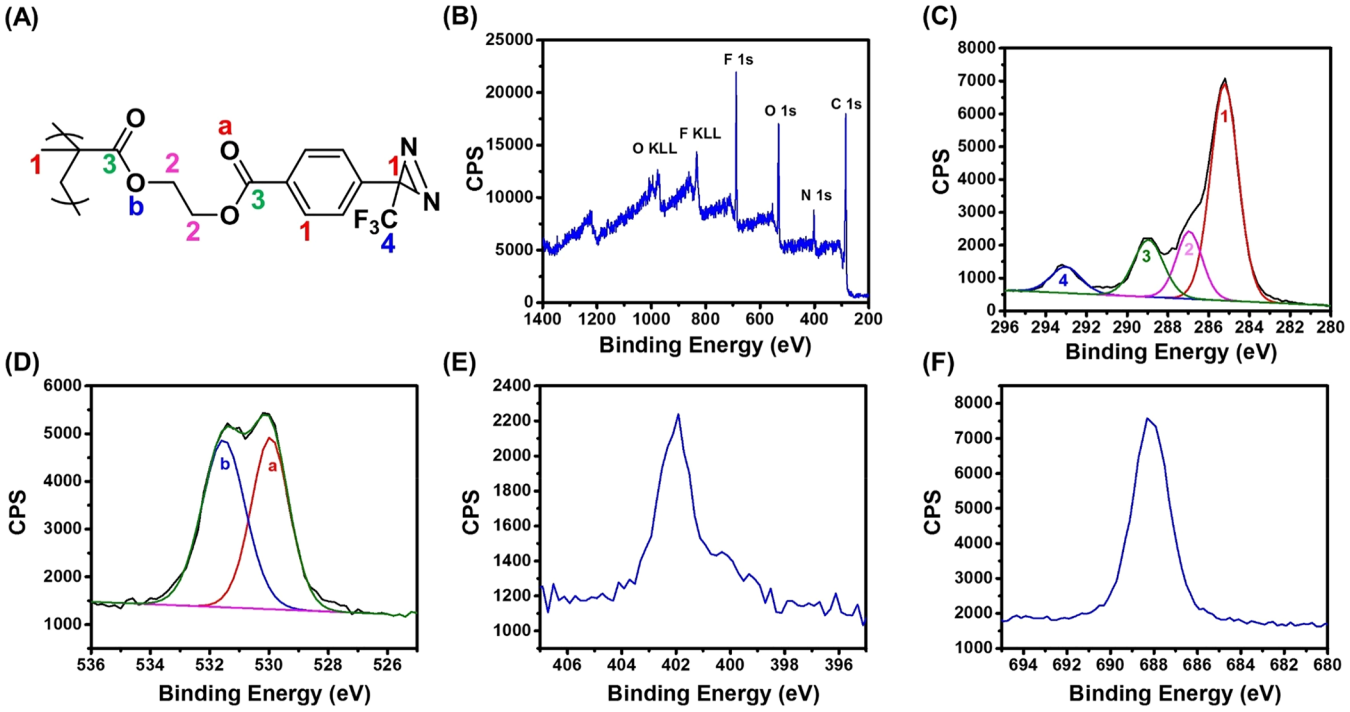

Figure 5. (A) Chemical structure of a TFMDA-functionalized PHEMA brush; (B) XPS survey scan; (C) C_{1s} high resolution spectrum; (D) O_{1s} high resolution spectrum; (E) N_{1s} high resolution spectrum; and (F) F_{1s} high-resolution spectrum of a TFMDA-functionalized PHEMA brush-coated substrate.

allows to facilitate adhesion with meniscus tissue, there are also several limitations to this strategy. The most significant drawback of the approach presented above is that the generation of tissue reactive aldehyde groups requires the use of short wavelength (~250 nm) UV−C type light, which does not only help to transform the polymer brush side chain functional groups, but, as discussed above, also leads to extensive photodegradation of the polymer brush. In addition, this part of the UV light spectrum is also the region that is most harmful to tissue and cells.[48,49] Another potential limitation of the direct UV-irradiation of PHEMA brushes is that the aldehyde groups that are generated react with amine groups present in the tissue to form imine bonds, which in principle are reversible in aqueous media.[50] Alternative chemistries may allow to facilitate the application of these coatings in wet environments. As an alternative bioadhesive coating platform, PHEMA brushes containing side chain diazirine moieties were investigated (Figure 4). Diazirines are attractive photoreactive groups to generate bioadhesives since they can be activated with relative long wavelength UV-light[51] and upon irradiation generate carbene groups that can insert in C−H, N−H, and O−H bonds.[52−54] The diazirine-functionalized brushes investigated in this study were prepared by DCC/DMAP-mediated coupling of TFMDA to PHEMA precursor brushes with thicknesses of 110 and 218 nm.

The introduction of the TFMDA side chain functional groups was monitored with XPS, UV−vis and FTIR spectroscopy. Figure 5 shows the XPS survey scan as well as C_{1s}, O_{1s}, N_{1s}, and F_{1s} high resolution spectra recorded on a PHEMA brush with an initial film thickness of 218 nm, which was reacted with TFMDA in the presence of DCC and DMAP for 16 h. The C, O, and F atom percentages determined by XPS analysis of the postmodified brush, which are listed in the Supporting Information, Table S1, indicate quantitative

DOI: 10.1021/acs.biomac.9b01196
Biomacromolecules 2020, 21, 240−249

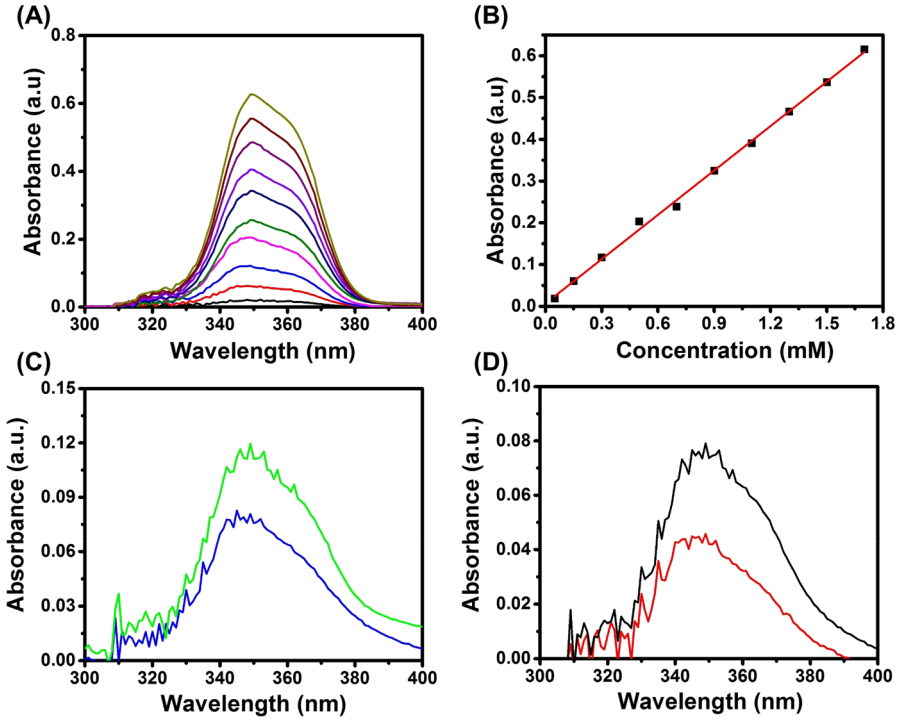

Figure 6. (A) UV−vis absorbance spectra of DCM solutions of TFMDA with concentrations of 0.05 mM (black), 0.15 mM (red), 0.3 mM (blue), 0.5 mM (pink), 0.7 mM (olive), 0.9 mM (navy), 1.1 mM (violet), 1.3 mM (purple), 1.5 mM (wine), and 1.7 mM (dark yellow). (B) Experimental data and linear fitting curve of absorbance vs TFMDA concentration. (C) UV−vis absorbance spectra of 218 nm thick PHEMA brush-coated fused silica substrates incubated in TFMDA DCM solution for 1 h (blue) and 16 h (green). (D) UV−vis absorbance spectra of 110 nm thick PHEMA brush-coated fused silica substrates incubated in TFMDA DCM solution for 1 h (red) and 16 h (black).

Table 1. Ellipsometric Film Thicknesses and Side Chain Conversions of TFMDA-Functionalized PHEMA Brushes

PHEMA Brush	Dry film thickness (nm)	PHEMA-TFMDA Brush	Reaction time (h)	Dry film thickness (nm)	Amount of TFMDA groups (nmol)	Estimated amount of HEMA units (nmol)[a]	HEMA conversion (%)
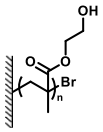	110.3±1.5	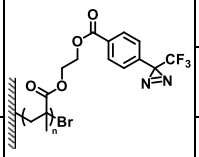	1	143.7±0.7	101	155	65%
			16	181.8±2.8	169	155	100%
	217.8±2.7		1	262.9±2.8	178	306	55%
			16	334.1±1.7	238	306	78%

[a]Calculated using the dry film thickness of the PHEMA brush, ρ = 1.15 g/cm^3, and the molecular weight of the HEMA repeating unit (130 g/mol).

substitution of the PHEMA side chains with TFMDA groups. The XPS N percentage, however, is lower than expected, which is attributed to partial degradation of the diazirine groups during the XPS analysis.[55] Since XPS only probes the top 10−20 nm of the brush film, UV−vis spectroscopy was used to estimate the total concentration of TFMDA moieties in the brushes. The TFMDA concentration in the polymer brushes was estimated using a calibration curve that was constructed using a series of TFMDA solutions in DCM with concentrations ranging from 0.05 to 1.7 mM (Figure 6A,B). To determine the TFMDA concentration, brushes grown from fused silica substrates were analyzed. Figure 6C,D shows UV−vis spectra of PHEMA brushes with initial film thicknesses of 218 nm (Figure 6C) and 110 nm (Figure 6D), which were reacted with TFMDA for 1 and 16 h. The TFMDA concentrations and percentages of conversion of HEMA side chain functional groups that were obtained from those spectra are summarized in Table 1. The results in Table 1 indicate that a reaction time of 16 h resulted in complete conversion of the HEMA side chain functional groups with TFMDA moieties in the thinner brush (d = 110 nm). Shortening the reaction time for the modification of the 110 nm thick polymer brush from 16 to 1 h decreases the conversion to 65%. For the thicker (218 nm) PHEMA brush, conversions of 55%, respectively, 78% were determined after reaction times of 1 and 16 h.

The adhesion of the TFMDA functionalized brushes toward meniscus tissue was studied using samples that were obtained from PHEMA brushes with initial film thicknesses of 110 or 218 nm, which were postmodified with TFMDA for 1 or 16 h. Figure 7A reports and compares the adhesion strengths of

DOI: 10.1021/acs.biomac.9b01196
Biomacromolecules 2020, 21, 240−249

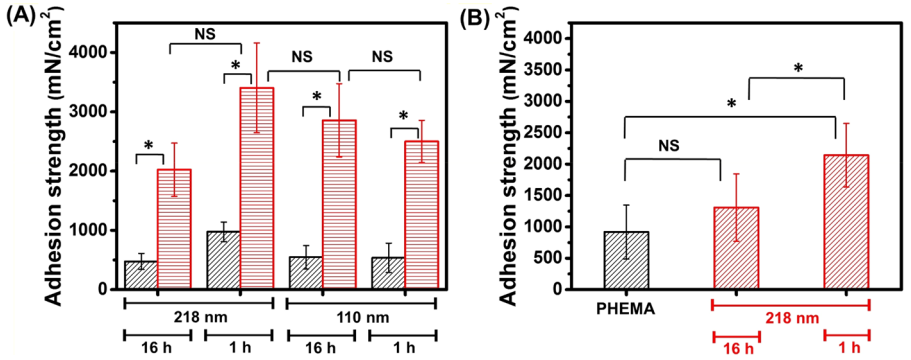

Figure 7. Adhesion strengths of (A) TFMDA-functionalized PHEMA brush-coated substrates with various thicknesses before (black) and after UV irradiation for 3 min (red). (B) PHEMA brush (black) and TFMDA-functionalized PHEMA brush coated substrates (red) treated with UV irradiation using a bandpass filter, which removes the 250 nm and allows for activation with only the 365 nm band, for 3 min. Asterisks indicate statistically significant differences, whereas NS represents the not significant difference between two conditions. Significant at $*p < 0.05$.

these 4 samples before and after UV irradiation for 3 min. Prior to UV-activation, the adhesion strengths of the TFMDA modified brushes are comparable to those of nonmodified PHEMA brushes before UV-irradiation (see Figure 2). UV-irradiation results in a significant increase in the adhesion strength. The adhesion strengths that are reported in Figure 7A are comparable to the results summarized in Figure 2. The results shown in Figure 7A, however, do not reveal any significant effects of the initial brush thickness or TFMDA concentration on the measured adhesion strength. This suggests that it is probably only the topmost layer of the TFMDA functionalized brush, where all of the HEMA repeating units are modified with TFMDA moieties according to the XPS analysis, which is involved in the formation of adhesive bonds with the meniscus tissue. It is important to note that the light source that was used to activate the brushes for the experiments that are summarized in Figure 7A extends into the UV−C region and contains a small band around 250 nm as well. As a consequence, the application of this range of UV wavelengths most likely leads to simultaneous generation of carbene moieties by photodecomposition of the diazirine groups as well as the formation of aldehyde groups by direct activation of the PHEMA brush. The adhesion strengths that are determined in these experiments thus reflect the contributions of both the carbene and the aldehyde groups. In a second experiment, in order to avoid direct activation of the PHEMA brush and to exclusively mediate adhesion using carbene moieties, the TFMDA-functionalized brushes were exposed to UV light using a bandpass filter that removes the 250 nm band and allows for exclusive activation with only 365 nm light. Figure 7B compares the adhesion strengths that were measured on a nonmodified PHEMA brush and two TFMDA-functionalized brushes that were UV-activated under these conditions for 3 min. The adhesion strength of the nonmodified PHEMA brush that is measured is comparable to those of the nonirradiated samples shown in Figure 2. This indicates that 365 nm UV-light does not lead to direct formation of tissue reactive groups in PHEMA brushes. In contrast, activation of the TFMDA modified brushes with 365 nm UV light results in an increase in the adhesion strength with the meniscus tissue. The covalent bonds that are formed and which contribute to tissue adhesion in this case are exclusively due to reaction of carbene moieties that are the product of the photodegradation of the diazirine groups.

CONCLUSIONS

Surface-initiated atom transfer radical polymerization has been used to produce thin, PHEMA brush coatings that can be transformed on-demand using UV-light as a trigger, from a nonadhesive to a tissue reactive state. Two strategies have been explored for the photochemical activation of the PHEMA brushes. A first strategy is based on direct UV-irradiation of PHEMA brush films, whereas the second approach involved the postpolymerization modification of the PHEMA side chain hydroxyl functional groups with 4-[3-(trifluoromethyl)-3*H*-diazirin-3-yl]benzoic acid. Adhesion experiments with meniscus tissue demonstrated that both polymer brush platforms upon UV-irradiation were able to create adhesive bonds with the tissue surface. While the direct irradiation of PHEMA brushes is very straightforward from an experimental point of view, this strategy relies on the 250 nm wavelength part of the UV spectrum. This short wavelength UV light unfortunately, not only generates the tissue reactive aldehyde groups, but also leads to extensive photodegradation of the polymer brush film. The diazirine containing brushes are comparably effective in terms of forming adhesive bonds with meniscus tissue. The activation of the diazirine groups, however, can be achieved using 365 nm wavelength UV light that does not lead to photodegradation. The proof-of-concept experiments presented in this manuscript have used silicon wafers and fused silica substrates as model surfaces. The versatility of SI-ATRP (and related grafting-from chemistries), however, will allow to apply this concept to a broader range of biomedically relevant surfaces.

ASSOCIATED CONTENT

Supporting Information

The Supporting Information is available free of charge on the ACS Publications website at DOI: 10.1021/acs.biomac.9b01196.

Radiant spectral distribution of the light source; Schematic of the adhesion testing setup; Photographs of different stages of an adhesion test on a representative PHEMA brush; Additional XPS characterization (PDF)

AUTHOR INFORMATION

Corresponding Author

*E-mail: harm-anton.klok@epfl.ch.

DOI: 10.1021/acs.biomac.9b01196
Biomacromolecules 2020, 21, 240−249

ORCID

Peyman Karami: 0000-0003-1098-4296
Dominique P. Pioletti: 0000-0001-5535-5296
Terry W. J. Steele: 0000-0001-8596-9619
Harm-Anton Klok: 0000-0003-3365-6543

Notes

The authors declare no competing financial interest.

■ ACKNOWLEDGMENTS

This work was financially supported by the Swiss National Science Foundation (SNSF) and China Scholarship Council (No. 201506360078).

■ REFERENCES

(1) Khanlari, S.; Dubé, M. A. Bioadhesives: A Review. *Macromol. React. Eng.* **2013**, *7*, 573−587.
(2) Mehdizadeh, M.; Yang, J. Design Strategies and Applications of Tissue Bioadhesives. *Macromol. Biosci.* **2013**, *13*, 271−288.
(3) Palacio, M. L.; Bhushan, B. Bioadhesion: a Review of Concepts and Applications. *Philos. Trans. R. Soc., A* **2012**, *370*, 2321−2347.
(4) Bouten, P. J.; Zonjee, M.; Bender, J.; Yauw, S. T.; van Goor, H.; van Hest, J. C.; Hoogenboom, R. The Chemistry of Tissue Adhesive Materials. *Prog. Polym. Sci.* **2014**, *39*, 1375−1405.
(5) Kaul, A.; Hutfless, S.; Le, H.; Hamed, S. A.; Tymitz, K.; Nguyen, H.; Marohn, M. R. Staple versus Fibrin Glue Fixation in Laparoscopic Total Extraperitoneal Repair of Inguinal Hernia: A Systematic Review and Meta-analysis. *Surg. Endosc.* **2012**, *26*, 1269−1278.
(6) Zhu, W.; Chuah, Y. J.; Wang, D.-A. Bioadhesives for Internal Medical Applications: A Review. *Acta Biomater.* **2018**, *74*, 1−16.
(7) Raja, P. R. Cyanoacrylate Adhesives: a Critical Review. *Rev. Adhesion Adhesives* **2016**, *4*, 398−416.
(8) Bhagat, V.; Becker, M. L. Degradable Adhesives for Surgery and Tissue Engineering. *Biomacromolecules* **2017**, *18*, 3009−3039.
(9) Trujillo-de Santiago, G.; Sharifi, R.; Yue, K.; Sani, E. S.; Kashaf, S. S.; Alvarez, M. M.; Leijten, J.; Khademhosseini, A.; Dana, R.; Annabi, N. Ocular Adhesives: Design, Chemistry, Crosslinking Mechanisms, and Applications. *Biomaterials* **2019**, *197*, 345−367.
(10) Ghobril, C.; Grinstaff, M. The Chemistry and Engineering of Polymeric Hydrogel Adhesives for Wound Closure: a Tutorial. *Chem. Soc. Rev.* **2015**, *44*, 1820−1835.
(11) Bré, L. P.; Zheng, Y.; Pêgo, A. P.; Wang, W. Taking Tissue Adhesives to the Future: From Traditional Synthetic to New Biomimetic Approaches. *Biomater. Sci.* **2013**, *1*, 239−253.
(12) Mogal, V.; Papper, V.; Chaurasia, A.; Feng, G.; Marks, R.; Steele, T. Novel On-Demand Bioadhesion to Soft Tissue in Wet Environments. *Macromol. Biosci.* **2014**, *14*, 478−484.
(13) Lang, N.; Pereira, M. J.; Lee, Y.; Friehs, I.; Vasilyev, N. V.; Feins, E. N.; Ablasser, K.; O'Cearbhaill, E. D.; Xu, C.; Fabozzo, A.; Padera, R.; Wasserman, S.; Freudenthal, F.; Ferreira, L. S.; Langer, R.; Karp, J. M.; del Nido, P. J. A Blood-Resistant Surgical Glue for Minimally Invasive Repair of Vessels and Heart Defects. *Sci. Transl. Med.* **2014**, *6*, 218ra6−218ra6a.
(14) Yang, Y.; Zhang, J.; Liu, Z.; Lin, Q.; Liu, X.; Bao, C.; Wang, Y.; Zhu, L. Tissue-Integratable and Biocompatible Photogelation by the Imine Crosslinking Reaction. *Adv. Mater.* **2016**, *28*, 2724−2730.
(15) Hong, Y.; Zhou, F.; Hua, Y.; Zhang, X.; Ni, C.; Pan, D.; Zhang, Y.; Jiang, D.; Yang, L.; Lin, Q.; Zou, Y.; Yu, D.; Arnot, D. E.; Zou, X.; Zhu, L.; Zhang, S.; Ouyang, H. A Strongly Adhesive Hemostatic Hydrogel for the Repair of Arterial and Heart Bleeds. *Nat. Commun.* **2019**, *10*, 2060.
(16) Shirzaei Sani, E.; Kheirkhah, A.; Rana, D.; Sun, Z.; Foulsham, W.; Sheikhi, A.; Khademhosseini, A.; Dana, R.; Annabi, N. Sutureless Repair of Corneal Injuries using Naturally Derived Bioadhesive Hydrogels. *Sci. Adv.* **2019**, *5*, No. eaav1281.
(17) Walker, B. W.; Lara, R. P.; Yu, C.; Sani, E. S.; Kimball, W.; Joyce, S.; Annabi, N. Engineering a Naturally-Derived Adhesive and Conductive Cardiopatch. *Biomaterials* **2019**, *207*, 89−101.
(18) Feng, G.; Djordjevic, I.; Mogal, V.; O'Rorke, R.; Pokholenko, O.; Steele, T. W. Elastic Light Tunable Tissue Adhesive Dendrimers. *Macromol. Biosci.* **2016**, *16*, 1072−1082.
(19) Nanda, H. S.; Shah, A. H.; Wicaksono, G.; Pokholenko, O.; Gao, F.; Djordjevic, I.; Steele, T. W. Nonthrombogenic Hydrogel Coatings with Carbene-Cross-Linking Bioadhesives. *Biomacromolecules* **2018**, *19*, 1425−1434.
(20) Shah, A. H.; Pokholenko, O.; Nanda, H. S.; Steele, T. W. Non-Aqueous, Tissue Compliant Carbene-Crosslinking Bioadhesives. *Mater. Sci. Eng., C* **2019**, *100*, 215−225.
(21) Granskog, V.; Andrén, O. C. J.; Cai, Y.; González-Granillo, M.; Felländer-Tsai, L.; von Holst, H.; Haldosen, L.-A.; Malkoch, M. Linear Dendritic Block Copolymers as Promising Biomaterials for the Manufacturing of Soft Tissue Adhesive Patches Using Visible Light Initiated Thiol−Ene Coupling Chemistry. *Adv. Funct. Mater.* **2015**, *25*, 6596−6605.
(22) Barbey, R.; Lavanant, L.; Paripovic, D.; Schuwer, N.; Sugnaux, C.; Tugulu, S.; Klok, H.-A. Polymer Brushes via Surface-Initiated Controlled Radical Polymerization: Synthesis, Characterization, Properties, and Applications. *Chem. Rev.* **2009**, *109*, 5437−5527.
(23) Zoppe, J. O.; Ataman, N. C.; Mocny, P.; Wang, J.; Moraes, J.; Klok, H.-A. Surface-Initiated Controlled Radical Polymerization: State-of-the-Art, Opportunities, and Challenges in Surface and Interface Engineering with Polymer Brushes. *Chem. Rev.* **2017**, *117*, 1105−1318.
(24) Yu, Q.; Zhang, Y.; Wang, H.; Brash, J.; Chen, H. Anti-Fouling Bioactive Surfaces. *Acta Biomater.* **2011**, *7*, 1550−1557.
(25) Vaisocherová, H.; Brynda, E.; Homola, J. Functionalizable Low-Fouling Coatings for Label-Free Biosensing in Complex Biological Media: Advances and Applications. *Anal. Bioanal. Chem.* **2015**, *407*, 3927−3953.
(26) Xu, F. J.; Neoh, K. G.; Kang, E. T. Bioactive Surfaces and Biomaterials via Atom Transfer Radical Polymerization. *Prog. Polym. Sci.* **2009**, *34*, 719−761.
(27) Banerjee, I.; Pangule, R. C.; Kane, R. S. Antifouling Coatings: Recent Developments in the Design of Surfaces That Prevent Fouling by Proteins, Bacteria, and Marine Organisms. *Adv. Mater.* **2011**, *23*, 690−718.
(28) Hucknall, A.; Rangarajan, S.; Chilkoti, A. In Pursuit of Zero: Polymer Brushes That Resist the Adsorption of Proteins. *Adv. Mater.* **2009**, *21*, 2441−2446.
(29) Schüwer, N.; Klok, H.-A. A Potassium-Selective Quartz Crystal Microbalance Sensor Based on Crown-Ether Functionalized Polymer Brushes. *Adv. Mater.* **2010**, *22*, 3251−3255.
(30) Tugulu, S.; Silacci, P.; Stergiopulos, N.; Klok, H.-A. RGD—Functionalized Polymer Brushes as Substrates for the Integrin Specific Adhesion of Human Umbilical Vein Endothelial Cells. *Biomaterials* **2007**, *28*, 2536−2546.
(31) Bilgic, T.; Klok, H.-A. Oligonucleotide Immobilization and Hybridization on Aldehyde-Functionalized Poly (2-Hydroxyethyl Methacrylate) Brushes. *Biomacromolecules* **2015**, *16*, 3657−3665.
(32) Xu, D.; Yu, W. H.; Kang, E. T.; Neoh, K. G. Functionalization of Hydrogen-Terminated Silicon via Surface-Initiated Atom-Transfer Radical Polymerization and Derivatization of the Polymer Brushes. *J. Colloid Interface Sci.* **2004**, *279*, 78−87.
(33) Neises, B.; Steglich, W. Simple Method for the Esterification of Carboxylic Acids. *Angew. Chem., Int. Ed. Engl.* **1978**, *17*, 522−524.
(34) Alang Ahmad, S.; Hucknall, A.; Chilkoti, A.; Leggett, G. J. Protein Patterning by UV-Induced Photodegradation of Poly (oligo (ethylene glycol) methacrylate) Brushes. *Langmuir* **2010**, *26*, 9937−9942.
(35) Ducker, R. E.; Janusz, S.; Sun, S.; Leggett, G. J. One-Step Photochemical Introduction of Nanopatterned Protein-Binding Functionalities to Oligo (ethylene glycol)-Terminated Self-Assembled Monolayers. *J. Am. Chem. Soc.* **2007**, *129*, 14842−14843.
(36) Jeyachandran, Y.; Terfort, A.; Zharnikov, M. Controlled Modification of Protein-Repelling Self-Assembled Monolayers by Ultraviolet Light: The Effect of the Wavelength. *J. Phys. Chem. C* **2012**, *116*, 9019−9028.

DOI: 10.1021/acs.biomac.9b01196
Biomacromolecules 2020, 21, 240−249

(37) Reynolds, N. P.; Tucker, J. D.; Davison, P. A.; Timney, J. A.; Hunter, C. N.; Leggett, G. J. Site-Specific Immobilization and Micrometer and Nanometer Scale Photopatterning of Yellow Fluorescent Protein on Glass Surfaces. *J. Am. Chem. Soc.* **2009**, *131*, 896−897.
(38) Tizazu, G.; el Zubir, O.; Patole, S.; McLaren, A.; Vasilev, C.; Mothersole, D. J.; Adawi, A.; Hunter, C. N.; Lidzey, D. G.; Lopez, G. P.; Leggett, G. J. Micrometer and Nanometer Scale Photopatterning of Proteins on Glass Surfaces by Photo-Degradation of Films Formed From Oligo (Ethylene Glycol) Terminated Silanes. *Biointerphases* **2012**, *7*, 54.
(39) Ul-Haq, E.; Patole, S.; Moxey, M.; Amstad, E.; Vasilev, C.; Hunter, C. N.; Leggett, G. J.; Spencer, N. D.; Williams, N. H. Photocatalytic Nanolithography of Self-Assembled Monolayers and Proteins. *ACS Nano* **2013**, *7*, 7610−7618.
(40) Pranantyo, D.; Xu, L. Q.; Neoh, K.-G.; Kang, E.-T.; Ng, Y. X.; Teo, S. L.-M. Tea Stains-Inspired Initiator Primer for Surface Grafting of Antifouling and Antimicrobial Polymer Brush Coatings. *Biomacromolecules* **2015**, *16*, 723−732.
(41) Feng, W.; Brash, J. L.; Zhu, S. Non-Biofouling Materials Prepared by Atom Transfer Radical Polymerization Grafting of 2-Methacryloloxyethyl Phosphorylcholine: Separate Effects of Graft Density and Chain Length on Protein Repulsion. *Biomaterials* **2006**, *27*, 847−855.
(42) Iwata, R.; Suk-In, P.; Hoven, V. P.; Takahara, A.; Akiyoshi, K.; Iwasaki, Y. Control of Nanobiointerfaces Generated From Well-defined Biomimetic Polymer Brushes for Protein and Cell Manipulations. *Biomacromolecules* **2004**, *5*, 2308−2314.
(43) Bochyńska, A. I.; Van Tienen, T. G.; Hannink, G.; Buma, P.; Grijpma, D. W. Development of biodegradable hyper-branched tissue adhesives for the repair of meniscus tears. *Acta Biomater.* **2016**, *32*, 1−9.
(44) Bochyńska, A. I.; Hannink, G.; Grijpma, D. W.; Buma, P. Tissue adhesives for meniscus tear repair: an overview of current advances and prospects for future clinical solutions. *J. Mater. Sci.: Mater. Med.* **2016**, *27*, 85.
(45) Bochyńska, A. I.; Hannink, G.; Buma, P.; Grijpma, D. W. Adhesion of tissue glues to different biological substrates. *Polym. Adv. Technol.* **2017**, *28*, 1294−1298.
(46) Hu, Y.; Goodeal, N.; Chen, Y.; Ganose, A. M.; Palgrave, R. G.; Bronstein, H.; Blunt, M. O. Probing the Chemical Structure of Monolayer Covalent-Organic Frameworks Grown via Schiff-Base Condensation Reactions. *Chem. Commun.* **2016**, *52*, 9941−9944.
(47) Di Giovannantonio, M.; Kosmala, T.; Bonanni, B.; Serrano, G.; Zema, N.; Turchini, S.; Catone, D.; Wandelt, K.; Pasini, D.; Contini, G.; Goletti, C. Surface−Enhanced Polymerization via Schiff-Base Coupling at the Solid−Water Interface under pH Control. *J. Phys. Chem. C* **2015**, *119*, 19228−19235.
(48) Brash, D. E.; Rudolph, J. A.; Simon, J. A.; Lin, A.; McKenna, G. J.; Baden, H. P.; Halperin, A. J.; Ponten, J. A Role for Sunlight in Skin Cancer: UV-Induced p53 Mutations in Squamous Cell Carcinoma. *Proc. Natl. Acad. Sci. U. S. A.* **1991**, *88*, 10124−10128.
(49) Ananthaswamy, H. N.; Pierceall, W. E. Molecular Mechanisms of Ultraviolet Radiation Carcinogenesis. *Photochem. Photobiol.* **1990**, *52*, 1119−1136.
(50) Ritter, E.; Przybylski, P.; Brzezinski, B.; Bartl, F. Schiff Bases in Biological Systems. *Curr. Org. Chem.* **2009**, *13*, 241−249.
(51) Halloran, M. W.; Lumb, J.-P. Recent Applications of Diazirines in Chemical Proteomics. *Chem. - Eur. J.* **2019**, *25*, 4885−4898.
(52) Preston, G. W.; Wilson, A. J. Photo-Induced Covalent Cross-Linking For the Analysis of Biomolecular Interactions. *Chem. Soc. Rev.* **2013**, *42*, 3289−3301.
(53) Murale, D. P.; Hong, S. C.; Haque, M. M.; Lee, J.-S. Photo-Affinity Labeling (PAL) in Chemical Proteomics: a Handy Tool to Investigate Protein-Protein Interactions (PPIs). *Proteome Sci.* **2016**, *15*, 14.
(54) Hermanson, G. T. The Reactions of Bioconjugation. *Bioconjugate Techniques*; Academic Press, 2013; Chapter 3, p 256.
(55) Léonard, D.; Chevolot, Y.; Bucher, O.; Sigrist, H.; Mathieu, H. J. ToF-SIMS and XPS Study of Photactivatable Reagents Designed for Surface Glycoengineering. Part I. N-(m-(3-(trifluoromethyl)diazirine-3-yl)phenyl)-4-maleimido-butyramide (MAD) on Silicon, Silicon Nitride and Diamond. *Surf. Interface Anal.* **1998**, *26*, 783−792.

DOI: 10.1021/acs.biomac.9b01196
Biomacromolecules 2020, 21, 240−249